

Adsorption of Fibrinogen onto Macroporous, Biocompatible Sponges Based on Poly(2-hydroxyethyl methacrylate)

A. K. Bajpai,¹ D. D. Mishra²

¹Bose Memorial Research Laboratory, Department of Chemistry, Government Autonomous Science College, Jabalpur (MP) 482 001, India

²Department of Chemistry, Shri Ram Institute of Technology, Marhotal, Jabalpur (MP) 482 002, India

Received 8 November 2005; accepted 19 January 2006

DOI 10.1002/app.24127

Published online in Wiley InterScience (www.interscience.wiley.com).

ABSTRACT: Hydrophilic, spongy matrices of poly(2-hydroxyethyl methacrylate) were synthesized by a redox polymerization method, and the adsorption of fibrinogen was carried out on their surfaces. The prepared sponges were characterized with Fourier transform infrared and environmental scanning electron microscopy and were assayed for their water-sorption potential. The chemical architecture of the sponges had a pronounced impact on both the water sorption and the protein adsorption affinity of the sponge surface. The adsorption kinetics were investigated, and kinetic parameters such as the rate constants for adsorption and desorption and the penetrate rate constant were eval-

uated. The influence of experimental conditions such as the pH and temperature were observed on the adsorption profiles of fibrinogen. The prepared sponges were also judged for *in vitro* blood compatibility by methods such as blood-clot-formation and hemolysis-percentage tests. An attempt was also made to correlate the fibrinogen adsorption capacity of the sponge to its antithrombogenic response to static blood. © 2006 Wiley Periodicals, Inc. *J Appl Polym Sci* 102: 1341–1355, 2006

Key words: adsorption; biocompatibility; hydrogels; proteins; swelling

INTRODUCTION

The interaction of proteins with solid surfaces not only is a fundamental phenomenon but is also key to several important and novel applications. In the field of biomaterials, protein adsorption is the first step in the integration of an implanted device or material with tissue.^{1,2} For example, the adsorption of blood proteins, such as fibrinogen, fibronectin, or vitronectin, can influence the adhesion of leukocytes, macrophages, or platelets and ultimately lead to fibrous encapsulation.^{3,4} In nanotechnology, protein-surface interactions are pivotal for the assembly of interfacial protein constructs such as sensors, actuators, and other functional components at the biological/electronic junction. Of the numerous proteins available for investigation, fibrinogen has been studied most intensely because of its prominent role in coagulation^{5,6} and its ability to promote platelet adhesion.^{7,8} Several studies have suggested that fibrinogen mediates platelet activation via its direct interaction with the platelet receptors GP IIb/IIIa, GP Ib, and possibly $\alpha_x\beta_y$.⁹ There are three distinct sites in the fibrinogen molecule that have been implicated to

play a role in the binding of platelets. Two of them, the dodecapeptide (γ 400–411) and the RGPS sequence (A_x 572–575), which are located in the D-domain of the γ chain, are believed to be critical for platelet interaction with fibrinogen.¹⁰ Using monoclonal antibodies that bind to these functional regions, different groups have studied the accessibility of these sites when fibrinogen is adsorbed.¹¹ These observations suggest that certain conformations of adsorbed fibrinogen are more platelet-adhesive than others, and this leads to the possibility of creating a non-platelet-adhesive substrate.

Materials for use in blood-contacting devices often suffer from poor hemocompatibility in comparison with the natural endothelial vascular lining.¹² A synthetic surface with improved biocompatibility would greatly improve the efficacy of blood-contacting devices such as vascular grafts, heart valves, catheters, and heart pumps.¹³ Although a variety of synthetic polymers such as cuprophan,¹⁴ polysulfone,¹⁵ poly(ether imide), and polycarbonate blank copolymers¹⁶ have been attempted in various blood-polymer interaction studies, the problem of thrombus formation on the polymer surface has always been observed. This obviously hampers the clinical success of blood-contacting devices and makes it necessary to use anticoagulants.¹⁷ Because platelet adhesion/activation is mediated by adsorbed plasma proteins, it is essential to study the adsorption of proteins onto the polymer

Correspondence to: A. K. Bajpai (akbajpailab@yahoo.co.in).

surfaces before their possible uses as biomaterials for different specific applications. The adsorption profile of plasma proteins depends strongly on the physicochemical properties of the polymers, such as surface wettability, surface charge density, and hydrophilic/hydrophobic rates.¹⁸ Thus, a complete study of protein adsorption is highly desirable not only for gaining insights into the protein–polymer interaction but also for predicting the possibility of using the polymer as a biomaterial for short- and long-term applications.

One of the most significant synthetic polymers, finding the greatest ever number of biomedical and pharmaceutical applications, is poly(2-hydroxyethyl methacrylate) (PHEMA), the history of which dates back to 1934 when Woodhouse¹⁹ filed the patent without judging the remarkable water-sorption properties. However, after only 2 decades, the polymers of 2-hydroxyethyl methacrylate (HEMA) were recognized as promising biomaterials.²⁰ The literature is richly documented with extensive studies on PHEMA because of the high water content, nontoxicity, and favorable tissue compatibility, which lead to many biomedical applications. These applications include soft contact lenses,²¹ drug delivery systems,²² kidney dialysis membranes,²³ and artificial liver support systems.²⁴ The presence of a hydroxyl group and a carboxyl group on each repeat unit makes this polymer compatible with water, and the hydrophobic α -methyl groups and backbone impart hydrolytic stability to the polymer and support the mechanical strength of the polymer matrix.²⁵

Thus, being motivated by the vital role of protein adsorption in biomedical fields, we have investigated the adsorption of fibrinogen onto macroporous, spongy polymers of PHEMA and judged their antithrombogenic properties by *in vitro* methods.

EXPERIMENTAL

Materials

HEMA was obtained from Sigma–Aldrich Co. (Steinheim, Germany), and the monomer was freed from the inhibitor with a method discussed in the next section. The crosslinker used in the polymerization of HEMA was ethylene glycol dimethacrylate (EGDMA), which was obtained from Merck (Darmstadt, Germany) and used as received. Potassium persulfate (KPS) and potassium metabisulfite were from Loba Chemie (Mumbai, India) and were used as received. Ethylene glycol was used as a cosolvent. Fibrinogen (porcine plasma) was purchased from Sigma–Aldrich Co. and used without any pretreatment. All other chemicals used were of standard quality, and double-distilled water was used throughout the experiments.

Purification of the monomer

Because of the poor stability of HEMA, high purity of the monomer is essentially required in hydrogel synthesis as the presence of impurities may greatly affect the swelling characteristics of the end polymer. The degradation of the monomer during transportation and storage at ambient temperatures may result in increased levels of methacrylic acid (MAA) and the naturally occurring crosslinker EGDMA. As illustrated in Figure 1, the HEMA monomer readily undergoes three common reactions:

1. HEMA may hydrolyze at the ester linkage to form MAA and ethylene glycol.
2. Two molecules of HEMA may transesterify to form the crosslinker and ethylene glycol.
3. The monomer may polymerize at the double bond, resulting in an oligomer or polymer.

Although an inhibitor such as hydroquinone (300 ppm) is normally added to minimize the later reactions, ultra-purity is desired for producing reliable data.

The impurity of MAA in the HEMA monomer was removed through the stirring of the monomer with 15 wt % anhydrous sodium carbonate for 3 h at 24°C and then vacuum filtration through Whatman filter paper. The yield from an initial volume of 100 mL of HEMA was 89%.

The impurity of EGDMA was then removed first by dissolution of the previously treated monomer in three times its volume of distilled water. Four extractions were performed with 50 mL of a 1 : 1 (v/v) mixture of carbon tetrachloride and cyclohexane, and the layers were allowed to separate for 30 min between extractions. The organic layer containing EGDMA was discarded after each extraction. The aqueous phase was placed *in vacuo* to remove any remaining organic solvent. The HEMA was then salted out with 100 g of NaCl, dried with anhydrous sodium sulfate, and filtered.

The partially purified HEMA monomer was vacuum-distilled in the presence of 1 g of hydroquinone (added to prevent polymerization) at 60 mmHg. The monomer was collected at 45°C, with the distillation flask being heated in a water bath at 55°C. The collection flask was cooled in an ice/acetone bath, and the first and last fractions of the distillation product were discarded. After distillation, the pure HEMA was transferred to an opaque glass bottle and stored at 0°C until use.

Purity of HEMA

The purity of distilled HEMA was determined by high-pressure liquid chromatography (HPLC). A Beckman Gold 127 system (Fullerton, CA) equipped with an ultraviolet (UV) detector, 25 cm \times 4.6 mm i.d. separation columns (octadecylsilane; C₁₈), and a 5- μ m particle

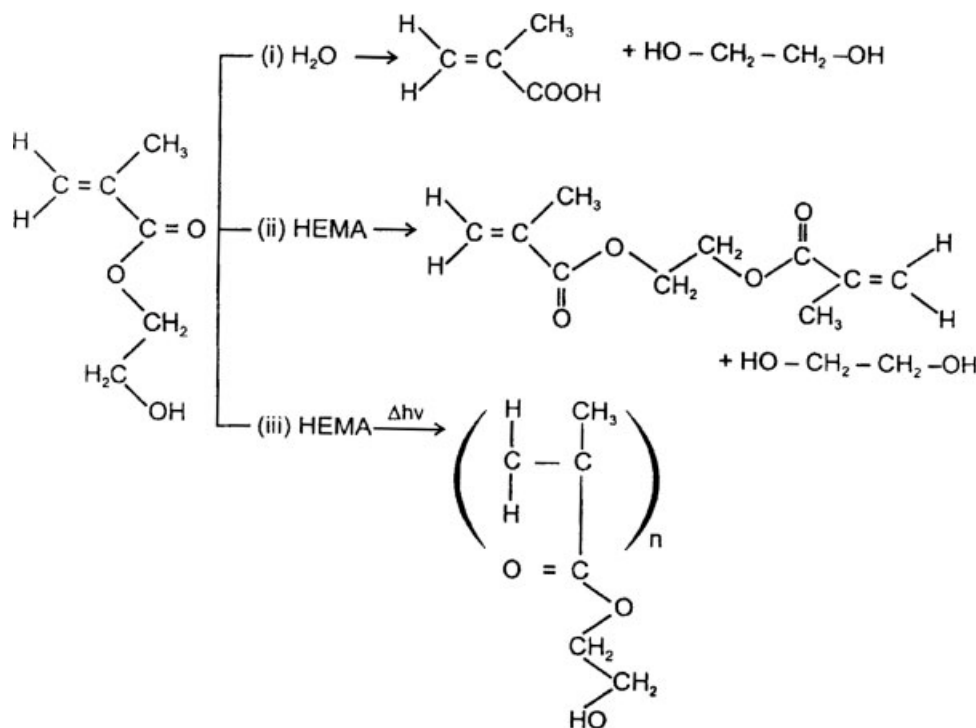


Figure 1 Synthesis of monomer HEMA.

size were used. The UV detector was set at 217 nm. The mobile phase was methanol–water (60 : 40 v/v), and the flow rate was kept at 1 mL/min. All samples were diluted with pure methanol to 1/1600. Samples (10 μL) were injected for each analysis. Samples of known concentrations of MAA and EGDMA were injected into the HPLC instrument, and the resultant chromatographs were used to construct a standard curve of known concentrations versus the area under the curve. The chromatograph showed three distinct peaks. The first peak at 3.614 min was identified as MAA. The next peak at 5.503 min was the major peak due to the HEMA monomer. The final peak at 15.3 min was due to the crosslinker EGDMA. The concentrations of the impurities in the monomer samples were less than 0.01 mol % MAA and 0.001 mol % EGDMA.

Synthesis of the PHEMA sponges

PHEMA sponges were synthesized by a redox polymerization method, as described elsewhere.²⁶ In a typical experiment, to a Petri dish (4-in. diameter; Corning, NY) were added HEMA (32.9×10^{-3} mol/L), ethylene glycol (71.6×10^{-3} mol/L) as a cosolvent, EGDMA (0.53×10^{-3} mol/L), and water. The amount of water was adjusted so that the total water content always exceeded the critical concentration. The whole reaction mixture was degassed with purging dry N_2 for 30 min. For initiating the polymerization reaction, a redox couple comprising degassed solutions of KPS (0.04 mol/L) and potassium metabisulfite (0.3×10^{-3}

mol/L) were added to the reaction mixture, and polymerization was allowed to proceed for 24 h. White, spongy gels of PHEMA were formed, which were allowed to swell in double-distilled water for a week. The swollen gels were cut into small, circular discs and allowed to dry at room temperature for a week. Upon drying, the gels changed into transparent buttons, which were stored in airtight containers. A series of PHEMA gels of various compositions were prepared and are summarized in Table I.

Swelling experiments

The dry gel sponges were allowed to swell in phosphate-buffered saline (PBS; pH 7.4) and were taken out after 7 days. Upon swelling, the gels again become spongy and white. The white, swollen gels were gently pressed between filter papers to remove excess water and weighed. The swelling ratio was calculated as follows:

$$\text{Swelling ratio} = W_s/W_d \quad (1)$$

where W_s and W_d are the swollen and dry weights of the sponges, respectively.

Adsorption experiments

The adsorption of fibrinogen onto the PHEMA sponges was performed by the batch contact process, as reported elsewhere.²⁷ Protein solutions for adsorption experiments were made in 0.5M PBS at a physi-

TABLE I
Water Sorption Capacity and Structural Parameters of PHEMA Sponges
of Various Compositions

HEMA (10 ³ mol/L)	EGDMA (10 ³ mol/L)	Initiator (10 ³ mol/L)	Water (%)	Swelling ratio	M _c	q (×10 ²)	v _e (×10 ⁻²⁰)
24.6	1.06	0.037	50	6.4	1186	10.9	5.66
32.9	1.06	0.037	50	7.4	1523	8.53	4.41
41.1	1.06	0.037	50	10.0	2734	4.75	2.45
49.3	1.06	0.037	50	11.2	3150	4.12	2.13
32.9	0.53	0.037	50	9.2	2254	5.76	2.98
32.9	1.06	0.037	50	7.4	1523	8.53	4.41
32.9	1.59	0.037	50	6.0	1290	10.07	5.26
32.9	2.12	0.037	50	4.4	653	19.9	10.2
32.9	1.06	0.037	50	7.4	1523	8.53	4.41
32.9	1.06	0.037	50	8.6	1998	6.50	3.36
32.9	1.06	0.111	50	9.8	2509	5.18	2.67
32.9	1.06	0.148	50	10.4	2815	4.61	2.38
32.9	1.06	0.148	50	7.4	1523	8.53	4.41
32.9	1.06	0.148	54	9.2	2254	5.76	2.98
32.9	1.06	0.148	62	10.0	2734	4.75	2.45
32.9	1.06	0.148	64	11.2	3150	4.12	2.13

ological pH of 7.4. A fresh solution of fibrinogen was always prepared for every adsorption experiment. Before the adsorption experiments, the PHEMA sponges were equilibrated in PBS for 72 h. The adsorption was then carried out by the gentle shaking of a solution of fibrinogen of a known concentration containing preweighed and fully swollen gels. The shaking was performed so gently that no froth was produced; otherwise, it would have formed an air–water interface. After a definite time period, the gels were removed, and the protein solution was assayed for the remaining concentration of fibrinogen spectrophotometrically (model 2201, Systronics, Ahmedabad, India). The adsorbed fibrinogen was calculated with the following mass–balance equation:

$$\text{Adsorbed fibrinogen } (\mu\text{g}/\text{cm}^2) = [(C_0 - C_e)V]/S \quad (2)$$

where C_0 and C_e are the initial and equilibrium concentrations of the fibrinogen solution ($\mu\text{g}/\text{mL}$), respectively; V is the volume of the protein solution; and S is the geometrical surface area of the swollen sponges, that is, the adsorbent.

For studying the kinetics of the adsorption process, the amount of adsorbed protein was determined at predetermined time intervals.

All the experiments were performed in triplicate, and an error of less than 1% was always obtained.

Blood-compatibility tests

A biomaterial is a substance used in prostheses or in medical devices designed for contact with the living body for the intended method of application and for the intended period. Synthetic polymers are widely used in both medical and pharmaceutical applications.

To be biocompatible, materials used in medical applications must meet certain criteria and regulatory requirements. The surfaces of biomaterials are believed to play an important role in determining biocompatibility. For materials that come in contact with blood, the formation of a clot is the most undesirable but frequently occurring event that puts restrictions on the clinical acceptance of a material as a biomaterial. Therefore, certain test procedures have evolved, and they need be employed to judge the hemofriendly nature of the biomaterials.

Clot-formation test

The antithrombogenic potential of the sponge surfaces was judged by the blood-clot-formation test, as described elsewhere.²⁸ In brief, the sponges were equilibrated with saline water (0.9% w/v NaCl) for 72 h in a constant-temperature bath. To these swollen gels were added 0.5 mL of acid citrate dextrose (ACD) blood followed by the addition of 0.03 mL of a CaCl₂ solution (4 mol/L) to start the thrombus formation. The reaction was stopped by the addition of 4.0 mL of deionized water, and the thrombus that formed was separated by soaking in water for 10 min at room temperature and then was fixed in a 36% formaldehyde solution (2.0 mL) for another 10 min. The fixed clot was placed in water for 10 min, and after it dried, its weight was recorded. The same procedure was repeated for the glass surface and sponges of various compositions, and the respective weights of the thrombi that formed were recorded.

Hemolysis assay

Hemolysis experiments were performed on the surfaces of the prepared sponges as described elsewhere.²⁹

In a typical experiment, a dry PHEMA film (4 cm²) was equilibrated in normal saline water (0.9% NaCl solution) for 24 h at 37°C, and human ACD blood (0.25 mL) was added to the spongy film. After 20 min, 2.0 mL of saline was added to the sponge to stop hemolysis, and the sample was incubated for 60 min at 37°C. Positive and negative controls were obtained by the addition of 0.25 mL of human ACD blood and a saline solution, respectively, to 2.0 mL of double-distilled water. The incubated sample was centrifuged for 45 min, the supernatant was taken, and its absorbance was recorded on a spectrophotometer at 545 nm. The percentage of hemolysis was calculated with the following relationship:

$$\text{Hemolysis (\%)} = \frac{(A_{\text{test sample}} - A_{(-)\text{control}})}{(A_{(+)\text{control}} - A_{(-)\text{control}}} \quad (3)$$

where A is the absorbance. The absorbance of positive and negative controls was 1.764 and 0.048, respectively.

Fourier transform infrared (FTIR) spectra

The IR spectrum of a dry sponge was recorded on a PerkinElmer Paragon 1000 spectrophotometer (Wellesley, MA). For this purpose, a film 0.1 cm thick was prepared, and the spectrum was recorded.

Environmental scanning electron microscopy (ESEM)

As no sample preparation is required in the ESEM technique, both the dry and swollen sponges were examined on a Philips XL30 ESEM instrument.

Statistical analysis

All presented adsorption results were expressed as an average of at least four independent determinations, and these mean values were used in plotting different curves.

RESULTS AND DISCUSSION

Characterization of the sponges

Structural parameters

An important structural parameter characterizing crosslinked polymers is M_c , the average molar mass between crosslinks, which is directly related to the crosslink density. The magnitude of M_c significantly affects the physical and mechanical properties of crosslinked polymers, and its determination has great practical value. Equilibrium swelling is widely used to determine M_c . Early research by Flory and

Rehner³⁰ laid the foundation for the analysis of equilibrium swelling. According to the theory of Flory and Rehner, for a network

$$M_c = -V_1 d_p \{ (v_s^{1/3} - v_{s/2}) / [\ln(1 - v_s) + v_s + \gamma v_s^2] \} \quad (4)$$

where V_1 is the molar volume of water (mL/mol), d_p is the polymer density (g/mL), v_s is the volume fraction of the polymer in the swollen sponge, and γ is the Flory–Huggins interaction parameter between the solvent and polymer.

The swelling ratio (weight of swollen sponge/weight of dry sponge) is equal to $1/v_s$. Here the crosslink density is defined as the molar fraction of crosslinked units (q):

$$q = M_0/M_c \quad (5)$$

where M_0 is the molar mass of the repeat unit.

Some authors define the crosslink density as the number of elastically effective chains totally included in a network per unit of volume (v_e). v_e is simply related to q because

$$v_e = d_p N_A / M_c \quad (6)$$

where N_A is Avogadro's number.

d_p was determined to be 1.18 g cm⁻³. Other parameters such as V_1 and γ were taken from the literature. With eqs. (4)–(6), the values of M_c , q , and v_e were calculated for sponges of various compositions. The values are summarized in Table I.

Appearance

During the polymerization of HEMA, the phenomenon of phase separation occurs in the polymer system, and as a result, a white and soft material is formed, whereas in the dry state, the material becomes hard and transparent. The dry and swollen sponges are depicted in Figure 2.

FTIR spectral analysis

The IR spectrum of the sponge of PHEMA is shown in Figure 3. The presence of HEMA is confirmed by the observed absorption bands at 1729 (C—O stretching), 1163 (O—C—C stretching), 3439 (O—H stretching), and 1469 cm⁻¹ (O—H bending). The spectrum also shows an asymmetric C—H stretch of the methylene group at 2946 cm⁻¹.

ESEM Analysis

The ESEM images of both dry and swollen sponges are shown in Figure 4(a,b), respectively. Although the dry sponge presents a homogeneous surface, the

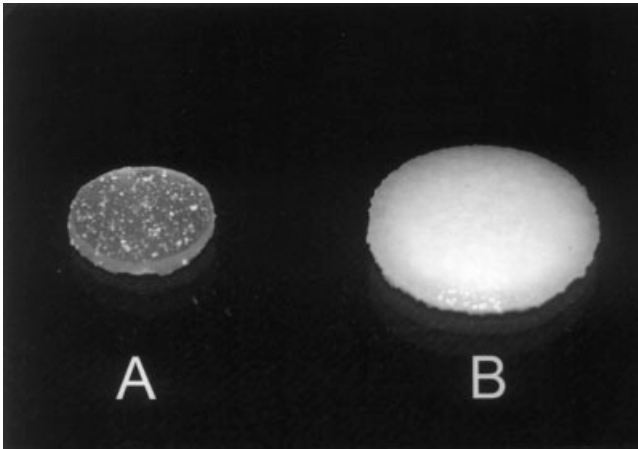


Figure 2 Photographs depicting (A) dry and (B) swollen PHEMA sponges.

morphology of the sponge significantly changes upon swelling. Figure 4(b) clearly reveals that macroporous domains varying in size between 6 to 10 μm developed because of the relaxation of macromolecular chains of PHEMA. The image also depicts some cracks about 6 μm wide produced by the relaxation of macromolecular chains.

Swelling of the PHEMA sponges

Because the biocompatibility of a material is also decided by its water content, the PHEMA sponges

of various compositions were synthesized and allowed to swell in PBS for 72 h. The water contents of the sponges are presented in Table I, and it is clear from the swelling ratio data that the water-sorption capacity of the sponges depended not only on the chemical architecture of the polymer but also on the amount of water present in the polymerization mixture.

The results summarized in Table I clearly reveal that the swelling ratio of the sponges increased with increasing water concentration in the range of 50–64% in the polymerization mixture. The increased swelling could be attributed to the fact that an increasing water concentration in the polymerization mixture increased the proportion of the nonsolvent, which facilitated the phase-separation process during polymerization. This obviously resulted in the formation of PHEMA sponges with larger interstitial void spaces, which were occupied by water molecules, thus enhancing the swelling.

The swelling ratio of the sponges was also influenced by the PHEMA content in the polymer. The table shows that when the amount of the monomer (HEMA) increased from 24.6 to 49.3 $\times 10^{-3}$ mol/L in the feed composition, the swelling ratio also increased. A possible explanation may be that for a given amount of water in the polymerization medium, increasing the HEMA content in the reaction mixture caused faster phase separation, thus producing PHEMA sponges of wider pore sizes. This

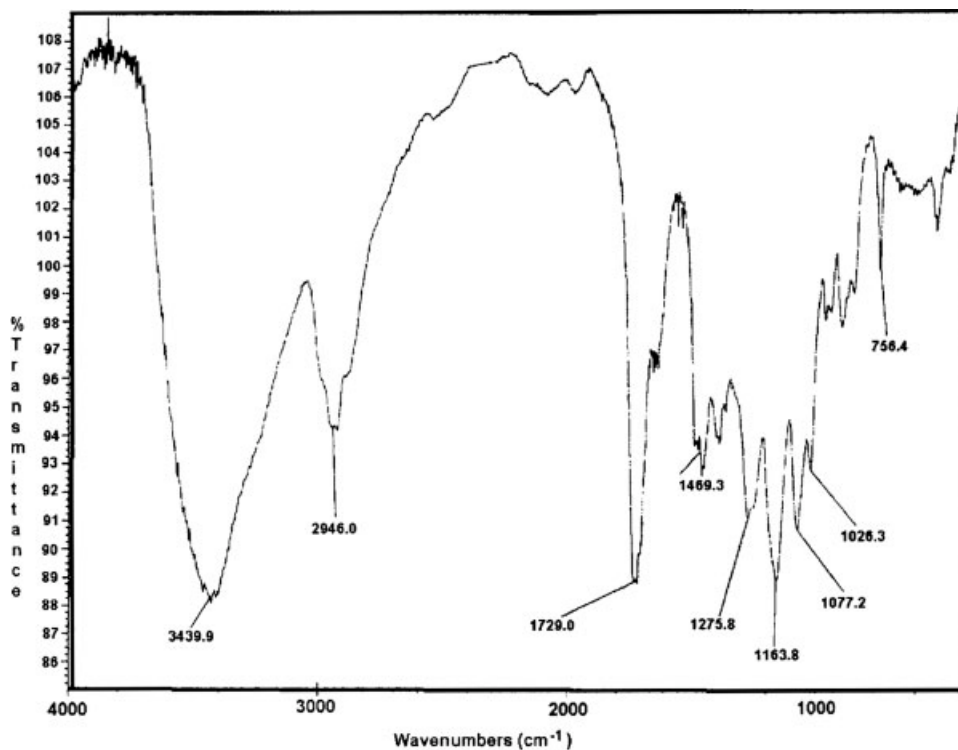


Figure 3 FTIR spectrum of the PHEMA sponge.

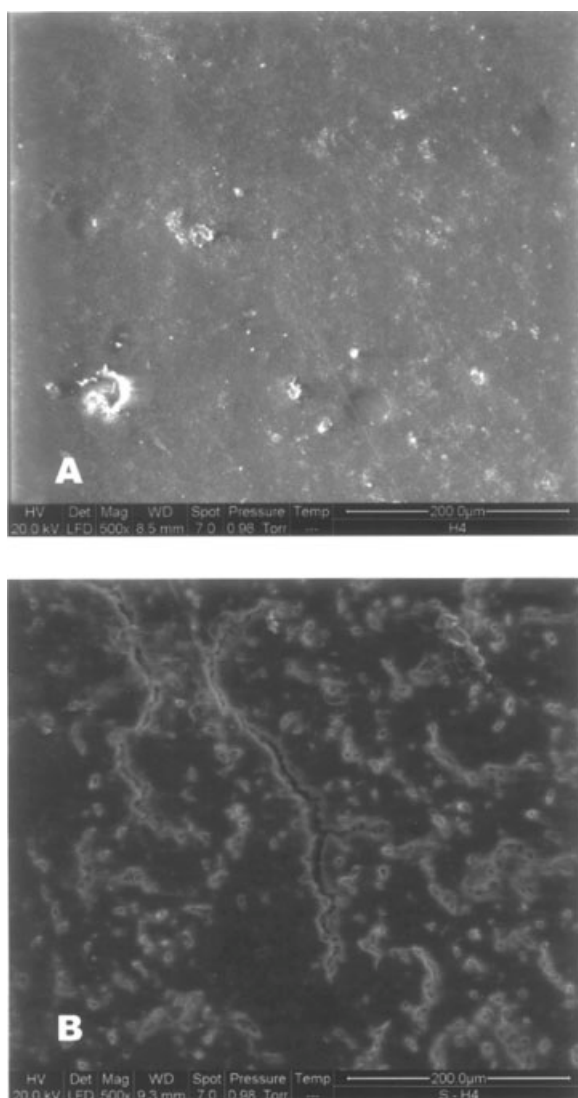


Figure 4 ESEM images of (a) dry and (b) swollen sponges.

obviously enhanced the degree of water sorption. Moreover, increasing the concentration of HEMA resulted in enhanced hydrophilicity of the sponge, which obviously brought about a rise in the water-sorption capacity.

The crosslinker had a pronounced effect on the swelling ratio of the sponges. When the EGDMA concentration was raised in the feed mixture in the range of $0.53\text{--}2.12 \times 10^{-3}$ mol/L, the degree of water sorption decreased; this is the usual finding. The observed decrease in the swelling ratio could be attributed to the fact that high amounts of the crosslinker (EGDMA) produced a compact network that increased the crosslink density of the sponges. Thus, because of the higher crosslink density, the pore sizes of the PHEMA sponges decreased, and this resulted in a lower degree of swelling. Another explanation for the observed fall in the swelling ratio of the PHEMA sponges is that the introduction of

the crosslinker increased the glass-transition temperature of the polymer, which obviously lowered the amount of water sorption.

The effect of the initiator concentration on the swelling ratio of PHEMA sponges was investigated by the variation of the amount of the initiator in the range of $0.037\text{--}0.148 \times 10^{-3}$ mol/L. The results presented in Table I indicate that with increasing initiator concentration, the swelling ratio also increased. A possible explanation may be that with increasing initiator concentration, a greater number of free radicals were generated with a large number of macroradical chains, thus enhancing the interstitial void space within the sponge. This obviously resulted in increased water sorption by the gel.

Modeling of the protein adsorption isotherms

Many protein adsorption modeling approaches have been tried, and several have been refined to be quite successful. Colloidal-scale models represent the protein as a particle and can accurately predict protein adsorption kinetics and isotherms. These colloidal-scale models include explicit Brownian dynamic type models,³¹ random sequential adsorption models,³² scaled particle theory,³³ slab models,³⁴ and molecular theoretical approaches.³⁵ Most of these approaches treat the electrostatics and van der Waals interactions between the protein and the surface and thus can capture dependences on the surface charge, protein dipole moment, protein size, or solution ionic strength.

Although the correlation between the adsorbed protein and bulk concentration of protein solutions has been handled with many adsorption isotherm equations,³⁶ the Langmuir equation has been the first choice of researchers because of its computational simplicity and ease of applicability to various adsorption data. In this study, two empirical equations have been used.

The Freundlich adsorption isotherm contains two parameters:

$$C_s = kC_b^{1/m} \quad (7)$$

The constant k is a measure of the capacity of the adsorption, and the exponent $1/m$ is a measure of the intensity of the adsorption.

The other equation is the linearized Langmuir equation:

$$\frac{C_b}{C_s} = \frac{C_b}{C_L} + \frac{1}{C_L}K \quad (8)$$

where C_b and C_s are the bulk and surface protein concentrations, respectively; C_L is the monotonically reached limiting surface concentration; and K is the

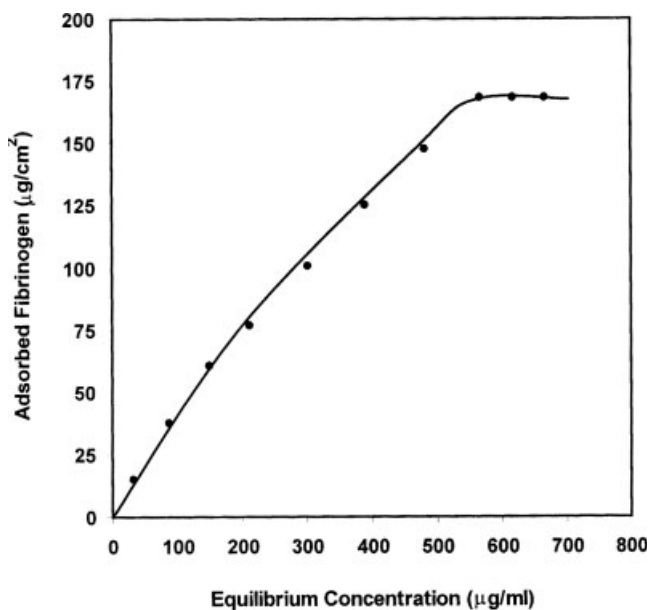


Figure 5 Adsorption isotherm of fibrinogen onto a PHEMA surface of a definite composition ([HEMA] = 32.9×10^{-3} mol/L, [EGDMA] = 1.06×10^{-3} mol/L, [Water] = 46.1%, [KPS] = 0.037×10^{-3} mol/L, [metabisulfite] = 0.40×10^{-3} mol/L, pH = 7.4, temperature = $27 \pm 0.2^\circ\text{C}$).

Langmuir constant, a parameter that describes the strength of the interaction between the protein and the surface.

Generally, proteins adsorb onto any surface with only a few exceptions. The fractional coverage is, therefore, strongly dependent on the bulk concentration of the proteins.

The effect of the initial concentration of the fibrinogen solution on the adsorbed amount of fibrinogen was investigated by the variation of its initial concentration in the range of 55–850 $\mu\text{g}/\text{mL}$. The results clearly indicate that the adsorbed amount gradually increased with an increasing concentration of the protein solution and ultimately attained a limiting value that was indicative of the formation of a monolayer on the PHEMA sponges. The observed increase could be attributed to the fact that with an increasing bulk concentration of the protein solution, a greater number of protein molecules arrived at the sponge–water interface and were adsorbed over the sponge surfaces.

More quantitative information about the protein–surface interaction could be obtained by the construction of an adsorption isotherm, which is normally obtained by the plotting of the adsorbed amount of fibrinogen against the residual concentration of the protein solution. The adsorption isotherm obtained in this case is shown in Figure 5, which shows a typical Langmuir type of curve that is characterized by an initially rising portion followed by a plateau portion. Similar types of isotherms have been frequently

reported in the literature.³⁷ The adsorption isotherm constants are summarized in Table II.

Effect of the pH and ionic strength

The pH of an adsorption medium has a significant influence on the amount of adsorbed protein. The effect is much more observable in those systems that involve ionic types of adsorbate and adsorbent surfaces. However, in this case, because the sponge was nonionic in nature, the effect of pH on adsorption was solely determined by the fibrinogen molecule, whose net charge varied with the pH of its solution. The effect of pH on the adsorption of fibrinogen was investigated by the variation of pH of the protein solution in the range of 2.1–11.0. The results are depicted later in Figure 7 and clearly imply that a maximum adsorption was obtained at pH 4.8, which was near the isoelectric point of fibrinogen (5.1). The optimum adsorption of proteins at their isoelectric points is a common phenomenon in protein–surface interactions.

The observed optimum adsorption of fibrinogen at the isoelectric point could have occurred because at the isoelectric point the lateral interactions between fibrinogen molecules were minimized and the protein acquired a compact conformation. Thus, a greater number of fibrinogen molecules could adsorb onto the given surface area of the PHEMA sponge.

An interesting feature revealed by Figure 6 is that the adsorption isotherms constructed for various ionic strengths responded differently to the pH of the adsorption medium. As the ionic strength increased, the maximum present in the isotherm became more and more pronounced. The observed results could be attributed to the fact that at a lower ionic strength, the density of the fibrinogen molecules at the IPN–solution interface was low and fewer protein molecules were operative at the active sites for adsorption. Thus, the lateral interactions among the molecules were not indifferent and significant below and above the isoelectric point of the protein. As a result, the adsorbed fibrinogen also did not vary appreciably, thus giving an isotherm with a less pronounced maximum. On the other hand, at a higher ionic strength, a greater number of fibrinogen molecules caused a greater degree of lateral interactions and, therefore, resulted in a pronounced maximum.

TABLE II
Static and Kinetic Constants for the Adsorption Process

Freundlich constants		K	k_1	k_2	k_A
k	($1/m$)	($\times 10^4$)	($\times 10^7 \mu\text{g}^{-1} \text{s}^{-1}$)	($\times 10^4 \text{s}^{-1}$)	($\times 10^7 \mu\text{g}^{-1}$)
2.30	0.95	1.9	6.0	9.2	6.4

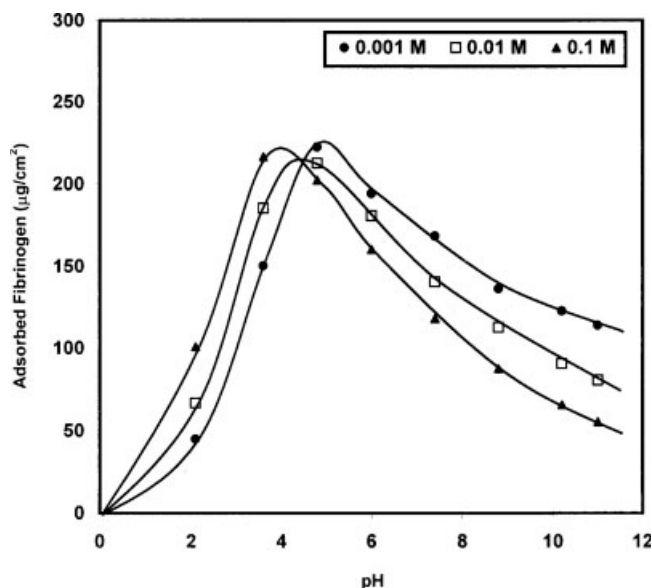


Figure 6 Adsorption isotherms of fibrinogen onto PHEMA sponges at different pHs and ionic strengths of the protein solutions with a fixed composition ([HEMA] = 32.9×10^{-3} mol/L, [EGDMA] = 1.06×10^{-3} mol/L, [Water] = 46.1%, [KPS] = 0.037×10^{-3} mol/L, [metabisulfite] = 0.40×10^{-3} mol/L, pH = 7.4, temperature = $27 \pm 0.2^\circ\text{C}$).

Another important observation is that the shape of the adsorption isotherm is appreciably affected by the ionic strength of the medium, as shown in Figure 6. It is implied by the results that in the acidic range the amount of adsorbed fibrinogen increased with the increasing ionic strength of the medium. The observed increase could have been due to the fact that with increasing ionic strength, the electrostatic repulsions decreased in the interior of the protein molecules, which led protein molecules to form more compact structures. Moreover, lateral repulsions between the adsorbed protein molecules also decreased with increasing ionic strength, and thus a greater number of molecules could adsorb onto the given surface area.

It is also revealed by Figure 6 that the maximum at which the adsorption of fibrinogen became optimum was slightly shifted toward an acidic pH range with increasing ionic strength. This shifting of the maximum has also been reported by other authors.³⁸

Dynamics of fibrinogen adsorption

Accurate knowledge of the adsorption kinetics under a given set of conditions is a prerequisite in elucidating the mechanisms of many fundamental biological processes. The adsorption of proteins from an aqueous solution onto a solid surface is normally considered to occur in three steps:³⁹ (1) the diffusion of protein molecules from the bulk to the interface, (2) the attachment of protein molecules to active sites

on the surface, and (3) the reformation of the structure of the protein molecule after adsorption. Of these steps, step 3 plays a significant role not only in controlling the adsorption kinetics of proteins but also in modifying the surface properties of the substrate.

The dynamics of the adsorption process were followed by the determination of the amounts of adsorbed fibrinogen at various time intervals, as shown in Figure 7. The rate of adsorption was almost constant up to 15 min and then gradually slowed, attaining a limiting value after 20 min. The kinetic profile of the adsorption process may be explained by the fact that the adsorption of functionalized large chains (e.g., proteins) is a two-regime process.⁴⁰ At the initial stages, the sponge surface was bare, and the kinetics of adsorption were governed by the diffusion of the chains from the bulk solution to the surface. All the fibrinogen molecules arriving at the interface were considered to be immediately adsorbed. The mass transport could be interpreted as Fickian diffusion. The diffusion coefficient (D) was determined with the following equation:

$$q = (2/\pi)C_0\sqrt{Dt} \quad (9)$$

From the slope of the curve drawn between q (adsorbed fibrinogen) and \sqrt{t} for fibrinogen solutions of various concentrations, the diffusion constants could be calculated, as summarized in Table III. With an increasing concentration of the fibrinogen solution, the diffusion constants constantly decreased.

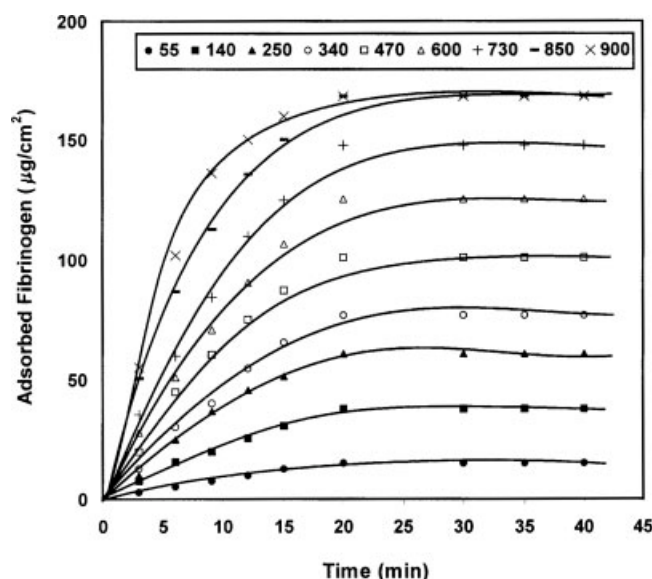


Figure 7 Plots showing the progress of the adsorption of fibrinogen onto PHEMA surfaces of a fixed composition ([HEMA] = 32.9×10^{-3} mol/L, [EGDMA] = 1.06×10^{-3} mol/L, [Water] = 46.1%, [KPS] = 0.037×10^{-3} mol/L, [metabisulfite] = 0.40×10^{-3} mol/L, temperature = $27 \pm 0.2^\circ\text{C}$).

TABLE III
Various Kinetic Parameters for the Adsorption of Fibrinogen onto PHEMA Sponges with Different Initial Bulk Concentrations of the Protein Solution

Fibrinogen ($\mu\text{g/mL}$)	D ($\times 10^5 \text{ cm}^2/\text{s}$)	τ ($\times 10^2 \text{ s}^{-1}$)
55	20.3	0.085
140	12.5	1.02
250	8.87	1.10
340	6.50	1.17
470	5.64	1.20
600	5.17	1.25
730	4.50	1.48
850	2.71	2.08

The observed decrease in the adsorbed mass of fibrinogen could be attributed to the fact that as the bulk concentration of the protein solution increased, the fibrinogen molecules approaching the substrate–solution interface had to go across a thicker protein layer near the interface and, therefore, diffuse slowly. A similar type of lower diffusion constant at a higher protein concentration has also been reported.⁴⁰ This was expected from the Ficks law of diffusion because the concentration gradient at the sponge–solution surface increased with an increase in the initial concentration of the fibrinogen solution.

In the later stage of the adsorption process, a barrier of adsorbed molecules exists, and the molecules arriving from solution have to diffuse across this barrier. This penetration is slow, and a theoretical treatment given by Ligorue and Leibler⁴¹ predicts an exponential time dependence for the later stages:

$$q(t) = q_{eq}[1 - \exp(-t/\tau)] \quad (10)$$

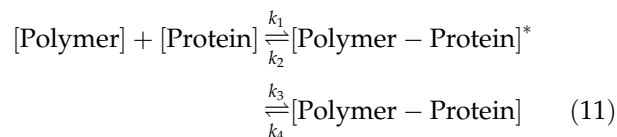
where q_{eq} is the adsorbed amount at equilibrium and $1/\tau$ is the penetration rate constant (τ is also known as the relaxation time). This equation suggests that the second process has an exponential nature, and the penetration rate may be obtained from the slope of the plot of $\ln(q_e - q)$ as a function of time. From the slopes of the straight lines (not shown), the $1/\tau$ values for various bulk concentrations of fibrinogen were calculated, and they are summarized in Table III.

The results clearly reveal that $1/\tau$ increased with increasing bulk and surface concentrations of fibrinogen. The observed increase was quite obvious because at higher bulk and surface concentrations, the protein molecules diffused more slowly and thus took greater time for penetration to be adsorbed onto the sponge surface.

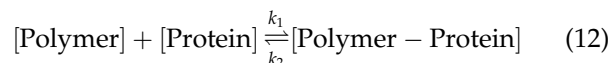
Kinetic model for adsorption

The kinetic model described by Tanaka et al.⁴² can be successfully employed to investigate the dynamic

nature of the adsorption process. In brief, the protein (fibrinogen) adsorption on the polymer surface (PHEMA sponge) can be described by the following equation:



where $[\text{Polymer} - \text{Protein}]^*$ represents the metastable complex composed of the polymer surface and the protein. In the early stage of protein adsorption, it is assumed that the reaction on the polymer surface can be simply described by the following equation, which reveals that the extent of adsorption depends on the amount of the complex:



On the basis of this equation, the production rate of the metastable complex can be given by the following equation:

$$\frac{d}{dt} [\text{Polymer} - \text{Protein}]^* = k_1 [\text{Polymer}] [\text{Protein}] - k_2 [\text{Polymer} - \text{Protein}]^* \quad (13)$$

where k_1 is the rate constant for adsorption and k_2 is the rate constant for desorption. The amount of the complex formed at time t is given by eq. (14):

$$[\text{Polymer} - \text{Protein}]_t^* = [\text{Polymer} - \text{Protein}]_\infty^* (1 - \rho)^{(-1/\tau)t} \quad (14)$$

where $[\text{Polymer} - \text{Protein}]_\infty^*$ is the concentration of the complex at theoretical time ∞ and τ is the relaxation time of the adsorption. The reciprocal of τ is defined by the following equation:

$$\tau^{-1} = k_1 [\text{Protein}]_0 + k_2 \quad (15)$$

where $[\text{Protein}]_0$ is the initial concentration of fibrinogen. The complete derivation of the equation can be seen in ref 42. Equation (15) clearly indicates that from the slope and intercept of the plot drawn between τ^{-1} and $[\text{Protein}]_0$, the values of k_1 , k_2 , and the association constant ($k_A = k_1/k_2$) can be calculated. In this study, the kinetic parameters calculated for fibrinogen adsorption are summarized in Table II and clearly indicate a lower affinity of fibrinogen molecules to the PHEMA sponge surfaces.

Effect of the concentration on the adsorption kinetics

The adsorption of fibrinogen is well known to exhibit different adsorption behaviors at low and high protein flux conditions,⁴³ thus indicating a history dependence on the ultimate surface coverage.⁴⁴ Initially, it was suggested that fibrinogen could exist in two distinct conformations on surfaces, resulting in two experimentally observable populations: a larger, irreversibly adsorbed layer on a smaller, reversibly adsorbed layer.⁴⁵ However, recent studies have revealed that fibrinogen can exist in many possible orientations and/or conformations depending on the adsorption history and the surface chemistry of the substrate.⁴³ It has also been shown that fibrinogen adsorbs nonspecifically to both hydrophobic and hydrophilic surfaces, resulting in a random mixture of end-on and side-on oriented molecules initially. After attachment to the surface, fibrinogen begins to increase its foot print (i.e., the number of segment-surface contacts) in a manner that is consistent with denaturation (unfolding) on hydrophobic surfaces and reorientation (rolling over) on hydrophilic surfaces. Thus, reversibly and irreversibly found populations may consist of many different protein footprint sizes, not only as two distinct conformations.

Thus, realizing the impact of protein flux on the adsorption dynamics of fibrinogen onto PHEMA sponge surfaces, we investigated the influence of the bulk concentration of the protein solution on the dynamic nature of the adsorption process by monitoring the progress of the adsorption process at different bulk concentrations varying in the range of 950–1200 $\mu\text{g}/\text{mL}$. The results shown in Figure 8 are quite unusual, and the adsorption profiles appear unlike any of those of other proteins. The results clearly reveal that although at low solution concentrations the adsorption reached a plateau value (Fig. 7), at higher concentrations, that is, from 950 to 1200 $\mu\text{g}/\text{mL}$, the adsorbed amount of fibrinogen attained an optimum value and thereafter decreased with increasing time. Similar results have been published elsewhere.⁴⁶ The results can be interpreted as follows.

The diffusion-controlled nature of the adsorption process, as discussed previously, reveals that each collision between a fibrinogen molecule and the sponge surface results in an adsorption event. The initial increase in adsorption with an increasing bulk concentration of the protein solution may obviously be due to the fact that a greater number of fibrinogen molecules interact with the surface and adsorb reversibly with end-on orientation. Because of the end-on orientation of adsorbed fibrinogen molecules, the footprint size becomes small, and consequently, less contact is established between the sponge surface and the adsorbed segments of the fibrinogen

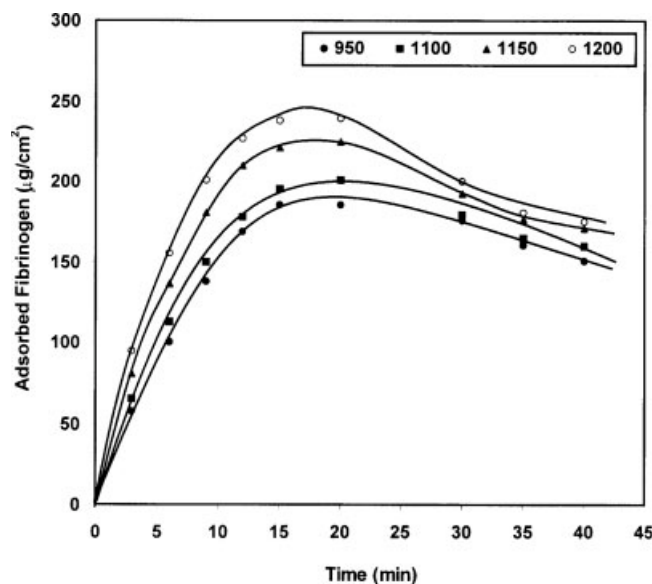


Figure 8 Plots showing the influence of higher concentrations of fibrinogen solutions on the progress of the adsorption of fibrinogen onto PHEMA sponges of a fixed composition ([HEMA] = 32.9×10^{-3} mol/L, [EGDMA] = 1.06×10^{-3} mol/L, [Water] = 46.1%, [KPS] = 0.037×10^{-3} mol/L, [metabisulfite] = 0.40×10^{-3} mol/L, temperature = $27 \pm 0.2^\circ\text{C}$).

molecule; this eventually results in reversible adsorption. It is well known that fibrinogen (molecular weight = 340,000–400,000 Da) is an exceptionally elongated molecule with an axial ratio (major axis/minor axis) of about 18:1. It contains about 10% charged residues and is negatively charged at pH 7.4 (isoelectric point ≈ 5.1).

Now, at a higher concentration (>900 $\mu\text{g}/\text{mL}$) of the protein solution, the adsorbed fibrinogen molecules are forced to undergo a conformational transition from end-on adsorption to side-on adsorption, so the footprint size of the adsorbed protein molecules increases. The increased contact with the sponge surface results in a firm binding to the surface, thus changing the adsorption from reversible adsorption to irreversible adsorption. Because of the side-on orientation of adsorbed fibrinogen molecules, the sponge surfaces are shielded from the other approaching molecules; therefore, the adsorbed amount of fibrinogen decreases. The whole scheme of adsorption can be modeled, as shown in Figure 9.

Effect of solutions and biological fluids

The influence of the solution and media on the adsorption of fibrinogen was examined with adsorption experiments in the presence of solutes such as potassium iodide (KI; 15% w/v), urea, and D-glucose (5% w/v) and in physiological fluids such as saline water (0.9% NaCl) and artificial urine. The adsorption

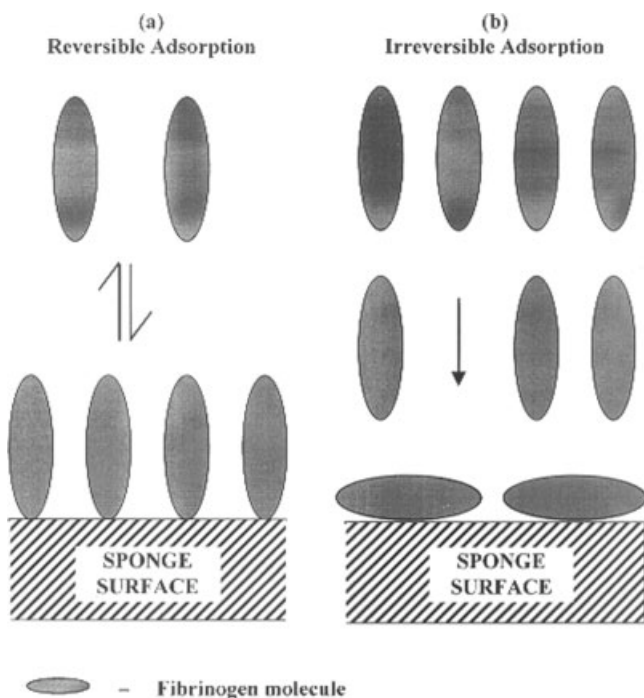


Figure 9 Hypothetical kinetic model depicting the mechanism of fibrinogen adsorption at (a) lower and (b) higher bulk concentrations of the protein solutions.

results are presented in Table IV and clearly reveal that in all cases, there was a fall in the adsorbed amount. The observed results could be explained as follows: the salt ions present in the adsorption media also competed with the adsorbing fibrinogen molecules and thus partially exhausted active sites on the sponge surfaces. This obviously resulted in a fall in the adsorption of fibrinogen.

Effect of the IPN composition on fibrinogen adsorption

The composition and organization of the adsorbed protein layer can be varied by numerous factors related to the substrate, such as the hydrophobicity, sorbed water content, microphase separation, and surface chemical functionality. As far as the chemistry of surfaces is concerned, the effect of the hydrophilic and hydrophobic balance of constituent chains in polymer surfaces has been found to play a key role in influencing the protein adsorption and subsequent platelet adhesion to the polymer.⁴⁷ In general, a hydrophobic surface offers greater affinity for protein adsorption than a hydrophilic surface, and this has been confirmed by a number of investigators also.⁴⁸ For example, surface grafting with tethered brushes of hydrophilic polymers, such as poly(ethylene glycol), has been shown to achieve minimal interaction with proteins and platelets.⁴⁹ Both flexibility and hydrophilicity are thought to play essential roles

in this reduced interaction of brushed surfaces with blood components because of a steric repulsion mechanism. On the other hand, the microarchitecture of material surface also affects the protein–material interaction substantially.

As mentioned previously, the presence of water is the decisive factor in the occurrence of phase separation because the thermodynamically unfavorable interaction between the water and polymer becomes dominant over other factors. This phase separation further results in a network consisting of contiguous, spherical particles surrounded by interconnected channels occupied by water.⁵⁰ With an increasing proportion of water in the polymerization mixture, the onset of phase separation becomes fast; therefore, the pore sizes of the PHEMA sponges decreased, whereas the swelling ratio increased. Thus, because of the observed increase in the water content of the sponges, the adsorption of fibrinogen was not favored,⁵¹ and a decrease in the adsorbed amount was obtained, as shown in Table V. The observed decrease can further be explained by the fact that with an increase in the initial dilution, the pore sizes of the polymer network also decreased, and this obviously restricted the free diffusion of protein molecules into the sponges, thereby reducing the amount of adsorbed protein.

In this study, the effect of the HEMA content in the sponges on the adsorbed amount of fibrinogen was investigated by the variation of the concentration of HEMA in the range of 24.6–49.3 $\times 10^{-3}$ mol/L. The results are shown in Table V and clearly imply that the amounts of adsorbed protein significantly decreased with increasing HEMA in the feed mixture of the sponges. The observed results could be explained by the fact that because of the hydrophilic nature of HEMA, its increasing concentration further enhanced the hydrophilicity of the polymer, which because of the greater water content, did not favor protein adsorption. The observed results were in agreement with the swelling results.

The crosslinking agent employed in this study was EGDMA, a known hydrophobic crosslinker. The

TABLE IV
Adsorption of Fibrinogen in Various Simulated Biological Fluids

Physiological fluid	Adsorbed amount ($\mu\text{g cm}^{-2}$)
PBS	168.4
KI (15% w/v)	158.6
Urea (5% w/v)	102.8
D-Glucose (5% w/v)	110.4
Saline water (0.9% w/v NaCl)	98.8
Synthetic urine ^a	92.6

^a NaCl (0.8% w/v), MgSO_4 (0.10% w/v), urea (21% w/v), and CaCl_2 (0.06% w/v).

TABLE V
Data Showing the Effects of Various Compositions of PHEMA Sponges and Water Contents on the Adsorbed Amount of Fibrinogen

Water (%)	HEMA (10 ³ mol/L)	EGDMA (10 ³ mol/L)	Adsorbed fibrinogen (μg/cm ²)
50	32.9	1.06	168
54	32.9	1.06	155
62	32.9	1.06	142
64	32.9	1.06	132
50	24.6	1.06	168
50	32.9	1.06	138
50	41.1	1.06	118
50	49.3	1.06	106
50	32.9	0.053	181
50	32.9	1.06	192
50	32.9	1.59	210
50	32.9	2.12	233

influence of EGDMA on the protein adsorption was investigated by an increase in its concentration in the range of $0.53\text{--}2.12 \times 10^{-3}$ mol/L. The results are shown in Table V and reveal that the adsorbed fibrinogen increased with increasing EGDMA concentration in the sponge. The increase in the protein adsorption could be attributed to the fact that the hydrophobic methylene groups of fibrinogen interacted with the crosslinker EGDMA and thus caused the adsorption of protein on the sponge surfaces as a result of hydrophobic interactions.⁵² Similar types of results have also been reviewed by other workers.⁵³ The water content is not the only important factor: the surface morphology⁵⁴ and volume restriction determine the state of water (degree of the free water fraction over restricted water), a critical factor influencing blood interactions at polymer surfaces. Therefore, it is imperative that a conclusion not be

drawn about biocompatibility on the basis of only the water content of polymers.

In vitro blood compatibility

Blood can be considered a flowing suspension of different kinds of cells in an aqueous solution of small solutes and more than 200 kinds of proteins. Upon injury or exposure to a foreign object, the clotting factors become activated and generate an enzyme called thrombin. Thrombin converts the soluble protein fibrinogen into insoluble fibrin. The formed fibrin acts as the foundation of a blood clot by providing a scaffold for the entrapment of platelets, blood cells, and plasma proteins.⁵⁵ Once a fibrin clot is formed, the clot itself can promote more clotting. Although this process is crucial to the healing of an open wound, it becomes problematic when it occurs in connection with the use of a blood-contacting medical device.

Thus, the correlation between the adsorbed protein and blood compatibility of the material must be explored to design a biomaterial with fair antithrombogenic properties. In this study, the thrombogenic response of the prepared PHEMA sponges to static blood was observed with the following two *in vitro* tests.

Blood-clot formation

The response of blood to contact with a material depends on physicochemical features such as the surface area, crystallinity, and hydrophobicity/hydrophilicity of the surface.⁵⁶ The blood-clot data obtained in this case are summarized in Table VI and clearly reveal the influence of the chemical com-

TABLE VI
Blood Compatibility Parameters of PHEMA Sponges of Different Compositions

HEMA (10 ³ mol/L)	EGDMA (10 ³ mol/L)	Initiator (10 ³ mol/L)	Water (%)	Weight of the blood clot (mg)	Hemolysis (%)
24.6	1.06	0.037	50	29.6	26.4
32.9	1.06	0.037	50	24.2	22.8
41.1	1.06	0.037	50	19.8	18.2
49.3	1.06	0.037	50	16.2	15.6
32.9	0.053	0.037	50	19.4	18.0
32.9	1.06	0.037	50	24.2	22.8
32.9	1.59	0.037	50	26.6	24.6
32.9	2.12	0.037	50	28.9	25.4
32.9	1.06	0.037	50	24.2	22.8
32.9	1.06	0.074	50	22.4	20.8
32.9	1.06	0.111	50	18.6	16.6
32.9	1.06	0.148	50	15.3	14.8
32.9	1.06	0.037	50	24.2	22.8
32.9	1.06	0.037	54	22.6	21.4
32.9	1.06	0.037	62	20.8	19.6
32.9	1.06	0.037	64	16.8	17.8
Glass surface	—	—	—	38.6	42.2

position of the sponge on the weights of the blood clot formed. When the concentration of HEMA was increased in the feed mixture of the sponge in the range of 24.6–49.3 mM, the weight of the blood clot significantly decreased. The observed fall could be attributed to the enhanced hydrophilicity of the sponge, which in turn resulted in decreasing adsorption of fibrinogen, which eventually lowered the amount of the clot formed.

The effect of increasing the crosslinker (EGDMA) concentration in the prepared sponges on the amount of the clot formed was investigated by increases in its concentration in the range of 0.53–2.12 mM. The results summarized in Table VI indicate an increase in the weight of the blood clot that formed with an increasing amount of the crosslinker. The results could be explained by the fact that because EGDMA is a hydrophobic crosslinker, its increasing content in the sponge enhanced the hydrophobicity of the matrix, which eventually produced more blood clotting on the surface.

In a similar way, a decrease in the weight of the blood clot was observed when the concentration of the initiator and water percentage were increased in the feed composition of the sponge. The observed decrease in the blood clot was in good agreement with the results of fibrinogen adsorption, which under both conditions showed a decreasing trend of protein adsorption.

Hemolysis percentage

The prepared sponges were also tested for hemolytic activity, and the results are shown in Table VI. They indicate that with increasing HEMA, initiator ($K_2S_2O_8$), and water concentrations in the feed mixture, the hemolysis percentage decreased, whereas an increasing concentration of the crosslinker (EGDMA) tended to cause more hemolysis of the blood on the sponge surface. The observed results were consistent with blood-clot-formation test results and led us to conclude that a material surface showing resistance to fibrinogen adsorption may prove to be more blood-compatible.

CONCLUSIONS

Macroporous, spongy materials were obtained when the HEMA monomer was polymerized by a redox system in the presence of a crosslinking agent (EGDMA) and a critical concentration of water. The macroporous nature was well confirmed by ESEM analysis. The water-sorption capacity of the sponge increased with increasing concentrations of the HEMA, initiator, and water in the feed composition,

whereas a fall was noticed with an increasing crosslinker content.

The adsorption of fibrinogen onto the sponge surfaces followed a Langmuir trend indicating a constant rise that further leveled off to a plateau. The adsorption was quite sensitive to the pH of the protein solution and showed an optimum at the isoelectric point of the protein (4.8). The optimum adsorption was further influenced by the ionic strength of the medium and shifted slightly to the acidic side with increasing ionic strength.

The bulk concentration of the protein solution greatly affected the dynamic nature of the adsorption, and a fall was noticed at later times when the protein flux was high. The lower adsorption at a later adsorption time was attributed to the conformational transition of adsorption from an end-on type to a side-on type.

The adsorption was also influenced by the chemical architecture of the PHEMA sponge. The increasing monomer, initiator, and water contents in the feed mixture gave rise to sponges displaying lower adsorption, whereas a highly crosslinked sponge adsorbed more fibrinogen.

The PHEMA sponges also displayed a fair level of blood compatibility, as confirmed by *in vitro* experiments with blood-clot formation and hemolysis. Although the macroporous sponges with greater PHEMA and water contents showed a higher antithrombogenic potential, the highly crosslinked sponge displayed poor thrombogenicity.

The authors gratefully acknowledge the authorities of the Indian Institute of Technology (Mumbai, India) for performing Fourier transform infrared and environmental scanning electron microscopy analysis of the prepared sponges.

References

1. Horbett, T. A. *Surf Sci Ser* 2003, 110, 393.
2. Gray, J. J. *Curr Opin Struct Biol* 2004, 14, 110.
3. Jahangir, A. R.; McClung, W. G.; Cornelius, R. M.; McCloskey, C. B.; Brash, J. L.; Santerre, J. P. *J Biomed Mater Res* 2002, 60, 135.
4. Shen, M.; Martinson, L.; Wanger, M. S.; Castner, D. G.; Ratner, B. D.; Horbett, T. A. *J Biomater Sci Polym Ed* 2002, 13, 357.
5. Wu, Y.; Simonovsky, F. I.; Ratner, B. D.; Horbett, T. A. *J Biomed Mater Res A* 2005, 74, 722.
6. Tzoneva, R.; Heuchel, M.; Groth, T.; Altankov, G.; Albrecht, W.; Paul, D. *J Biomed Sci Polym Ed* 2002, 13, 1033.
7. Lee, J. H.; Oh, S. H. *J Biomed Mater Res* 2002, 60, 44.
8. Tsai, W. B.; Grunkemeier, J. M.; Horbett, T. A. *J Biomed Mater Res A* 2003, 67, 1255.
9. Beguin, S.; Kumar, R. *Thromb Haemost* 1997, 78, 590.
10. Chinn, J. A.; Posso, S. E.; Horbett, T. A.; Ratner, B. D. *J Biomed Mater Res* 1991, 25, 535.
11. Grunkemeier, J.; Horbett, T. *J Mol Recognit* 1996, 9, 247.
12. Ratner, B. D. *J Biomed Mater Res* 1993, 27, 283.
13. Ratner, B. D.; Bryant, S. J. *Annu Rev Biomed Eng* 2004, 6, 41.

14. Klein, E. *Membr Sci* 1979, 5, 173.
15. Nishimura, T. In *Biomedical Application of Polymeric Materials*; Tsuruta, T.; Hyashi, T.; Kataoka, K.; Ishihara, K.; Kimura, Y., Eds.; CRC: Boca Raton, FL, 1993; p 191.
16. Konstantin, P.; Bailey, R. *Blood Purif* 1986, 4, 6.
17. Markwardt, F. *Thromb Haemost* 1991, 66, 141.
18. Vogler, E.; Graper, J.; Harper, G.; Sugg, H.; Lander, L.; Brittain, W. *Biomed Mater Res* 1995, 29, 1005.
19. Woodhouse, J. C. U.S. Pat. 2,129,722 (1938).
20. Dreiflis, M.; Klenka, L. *Csl Ofial* 1959, 15, 95.
21. Franklin, V. J.; Bright, A. M.; Tighe, B. J. *Trends Polym Sci* 1993, 1, 9.
22. Ruiz, J.; Mantecon, A.; Cadiz, V. *J Appl Polym Sci* 2002, 85, 1644.
23. Ragaller, M.; Werner, C.; Bleyl, J.; Adam, S.; Jacobasch, H.-J.; Albrecht, D. M. *Kidney Int* 1998, 53, S-84.
24. Mao, J.; Zhao, L.; de Yao, K.; Shang, Q.; Yang, G.; Cao, Y. *J Biomed Mater Res* 2003, 64, 301.
25. Refojo, M. F. *J Polym Sci Part A-1: Polym Chem* 1967, 5, 3103.
26. Lou, X.; Chirila, T. V.; Clayton, A. B. *Int J Polym Mater* 1997, 37, 1.
27. Bajpai, A. K.; Shrivastava, M. *J Macromol Sci Pure Appl Chem* 2001, 38, 1123.
28. Imai, Y.; Nose, Y. *J Biomed Mater Res* 1972, 6, 165.
29. Bajpai, A. K.; Saini, R. *Polym Int* 2005, 54, 1223.
30. Flory, P. J.; Rehner, J. *J Chem Phys* 1943, 11, 521.
31. Oberholzer, M. R.; Lenhoff, A. M. *Langmuir* 1999, 15, 3905.
32. Adamczyk, Z.; Weroniski, P.; Musial, E. *Colloids Surf A* 2002, 208, 29.
33. Brusatori, M. A.; Van Tassel, P. R. *J Colloid Interface Sci* 1999, 219, 333.
34. Stahlberg, J.; Jonsson, B. *Anal Chem* 1996, 68, 1536.
35. Fang, F.; Szleifer, I. *Biophys J* 2001, 80, 2568.
36. Roth, C. M.; Lenhoff, A. M. *Surf Sci Ser* 1998, 75, 89.
37. Kayirhan, N.; Denizli, A.; Hasirci, N. *J Appl Polym Sci* 2001, 81, 1322.
38. Bajpai, A. K. *Polym Int* 2004, 53, 261.
39. Dijit, J. C.; Cohen Stuart, M. A.; Hofman, J. F.; Fleer, G. J. *Colloids Surf* 1990, 51, 141.
40. Siqueria, D. F.; Breiner, U.; Stadler, R.; Stamm, M. *Langmuir* 1996, 12, 972.
41. Liguoro, C.; Leibler, L. *J Phys (Paris)* 1990, 51, 1313.
42. Tanaka, M.; Mochizaki, A.; Shiroya, T.; Motomura, T.; Shimura, K.; Onishi, M.; Okahata, Y. *Colloids Surf A* 2002, 203, 195.
43. Wertz, C. F.; Santore, M. M. *Langmuir* 2001, 17, 3006.
44. Wertz, C. F.; Santore, M. M. *Langmuir* 1999, 15, 8884.
45. MacRitchie, F. *J Colloid Interface Sci* 1972, 38, 484.
46. Wertz, C. F.; Santore, M. M. *Langmuir* 2002, 18, 706.
47. Grainger, D.; Okano, T.; Kim, S. W. In *Advances in Biomedical Polymers*; Gebelein, C. G., Ed.; Plenum: New York, 1987; p 229.
48. Kataoka, K.; Ito, H.; Amano, H.; Nagasaki, Y.; Kato, M.; Tsuruta, T.; Suzuki, K.; Okano, T.; Sakurai, Y. *J Biomater Sci Polym Ed* 1998, 9, 111.
49. Harris, J. M. In *Poly(ethylene glycol) Chemistry*; Harris, J. M., Ed.; Plenum: New York, 1992.
50. Chirila, T. V.; Higgins, B.; Dalton, P. D. *Cellul Polym* 1998, 17, 141.
51. Ratner, B. D.; Hoffman, A. S.; Hanson, S. R.; Harker, L. A.; Whiffen, J. D. *J Polym Sci Polym Symp* 1979, 66, 363.
52. Elbert, D. L.; Hubbell, J. A. *Annu Rev Mater Sci* 1996, 26, 365.
53. Wang, Y.-X.; Robertson, J. L.; Spillman, W. B.; Claus, R. O. *Pharm Res* 2004, 21, 1362.
54. Puleo, D. A.; Nanci, A. *Biomaterials* 1999, 20, 2311.
55. Vorman, L. *Blood; Natural History*: New York, 1967.
56. Vienken, J.; Diamantoglou, M.; Hahn, C.; Kamusewitz, H.; Paul, D. *Artif Organs* 1995, 19, 398.